J BONE ONCOL 51 (2025) 100664

Contents lists available at ScienceDirect

Journal of Bone Oncology

journal homepage: www.elsevier.com/locate/jbo

Faster R-CNN model for target recognition and diagnosis of scapular fractures☆

Qiong Fang [a,*], Anhong Jiang [b], Meimei Liu [a], Sen Zhao [a]

[a] Department of Basic Medicine, Anhui Medical College, Hefei 230601 Anhui, China
[b] Department of Radiology, The Second Affiliated Hospital of Anhui Medical University, Hefei 230601, China

HIGHLIGHTS

- The CNN model improved diagnostic accuracy for scapular fractures to 97.78% with orthopedist input vs. 82.95% without.
- CNN model with clinical expertise showed higher predictive value than traditional methods in distinguishing scapular fractures.
- The study highlights the CNN model's potential to enhance clinicians' ability to diagnose scapular fractures.

ARTICLE INFO

Keywords:
Convolutional neural network
Scapular fracture
Computed tomography
Computer-aided diagnosis

ABSTRACT

Objective: This study aims to establish a diagnostic model for scapular fractures using a convolutional neural network (CNN) and to discuss the clinical advantages of this model in diagnosing such complex conditions.
Methods: Computed tomography (CT) images of 90 patients with scapular fractures were collected. A faster R-CNN-based recognition model was developed and compared with manual diagnosis. External validation was conducted to evaluate the model's accuracy, sensitivity, specificity, positive predictive value, and negative predictive value.
Results: The CNN model, when combined with medical expert interpretation, demonstrated significantly higher specificity and positive predictive value compared to orthopedist-independent interpretation and algorithm-independent prediction ($P < 0.05$). The area under the curve (AUC) value of the combined approach was significantly higher than that of orthopedist-independent interpretation and algorithm-independent prediction groups, with statistically significant differences ($P < 0.05$). The accuracy of the CNN algorithm model combined with orthopedist interpretation was 97.78 %, significantly higher than orthopedist-independent interpretation (82.95 %) and CNN algorithm-independent prediction (92.05 %) ($P < 0.05$).
Conclusions: The CNN-based recognition model for scapular fractures can assist clinicians in improving their diagnostic accuracy and precision in identifying such fractures on CT images.

1. Introduction

Scapular fracture is a low-incidence fracture type, accounting for about 7–25 % of the total body fractures [1], mainly due to direct violence, and high-energy trauma, accompanied by other tissue injuries [2,3]. If it is not timely and effective treatment, it is easy to cause shoulder joint and upper limb dysfunction, which seriously affects the health of patients [4]. X-ray examination is the preferred method for clinical diagnosis of scapular fracture, but the tissue and anatomical position around the scapula are complicated, and X-ray can not clearly and comprehensively show the specific condition of the fracture, which is easy to miss and misdiagnose [5,6]. With the development of medical technology, multi-slice spiral CT has been widely used in clinical practice, which can accurately display the specific conditions of fractures [7]. For the bone injury of the fine structure of the scapula, although high-resolution CT is available, some concealed scapular fractures are still easy to miss and misdiagnosed in practice [8]. In addition, the interpretation of scapular radiographs requires a lot of time and requires the expert to have rich experience in reading the radiographs [9]. Therefore, finding an examination protocol with a high fracture

☆ This article is part of a special issue entitled: 'MI Orthopedics' published in Journal of Bone Oncology.

* Corresponding author.
E-mail address: fangqiong@ahyz.edu.cn (Q. Fang).

https://doi.org/10.1016/j.jbo.2025.100664
Received 30 June 2024; Received in revised form 3 December 2024; Accepted 7 February 2025
Available online 19 February 2025

recognition rate has an important impact on the treatment of this disease.

Fracture analysis [10], which includes procedures such as stiffness evaluation [11], or structural integrity [12–14], is crucial for evaluating the health of bones prior to surgical planning. The convolutional neural networks (CNN) model in deep learning is first tried and applied in the field of image classification and target recognition [15]. Due to its characteristics based on semantic recognition, the CNN model is gradually applied in imaging diagnosis [16,17]. In recent years, the study of fracture diagnosis using CNN model has been carried out constantly [18]. The CNN is a kind of feedforward neural network with convolutional computation and deep structure, which is one of the representative algorithms of deep learning and is widely used in the medical field because of its help in accurate diagnosis, reducing medical errors, and improving productivity [19]. In addition, the CNN has been successfully applied to the automatic classification of chest and limb CT [20,21].

Medical imaging of the human physiology has been a common practice for clinical diagnosis, and includes the analysis of these structures leading to more appropriate surgical plannings [22–25]. The imaging modalities involved computed tomography, magnetic resonance imaging, ultrasound, etc, and are usually coupled with image processing techniques [26–29] to enhance the diagnosis accuracy. Orthopedic fracture analysis, combined with CT-based multi-view semantic alignment [30,31] and deep incompleteness factorization techniques [32], is crucial for accurately assessing bone structural integrity and formulating treatment plans before surgery. The purpose of this study was to establish a fracture calibration and recognition model based on the CNN algorithm for scapular CT images and to explore its application value in assisting and improving diagnostic efficiency and accuracy. To assist surgeon in shortening the time of reading film, to improve diagnostic accuracy and work efficiency.

2. Materials and methods

2.1. Subject of study

The DICOM format images of shoulder CT scans of shoulder blade fractures admitted to our hospital from January 2020 to July 2023 were collected. After screening, 90 cases of data were selected for study. The patients ranged in age from 27 to 81 years. All patients signed informed consent forms. Fracture types of scapulars were recorded for all patients, including scapular neck, coracoid process, glenoid, acromion, scapular body, and scapular spine.

2.2. Imaging examination

All the images for training and testing in this study were collected by multi-slice spiral CT equipment in our hospital. The CT scan protocol was as follows: Patient was supine, spiral scan, scan area of the shoulder. Tube voltage 100 ~ 120 kV, tube current 50 ~ 200 mAs, scanning thickness 16 × 0.50 ~ 16 × 0.75 mm, pitch 0.7 ~ 0.9. The thinnest allowable layer thickness is 0.70 mm, and the recombination spacing is 0.35 mm (overlapping 50% recombination).

2.3. Construction of model

The CNN model adopts the classical Faster R-CNN network structure. The network structure of Faster R-CNN is divided into four parts: convolution layers (Conv) and region proposal network (region proposal network). RPN ROI pooling layer and classifier [33]. Faster R-CNN uses VGG16 with regular network structure. The workflow of target detection is shown in Fig. 1.

In Faster R-CNN, the role of ROI Pooling is to pool the corresponding area into a fixed-size feature map according to the position coordinates of the pre-selected frames, so as to facilitate subsequent classification and bounding box regression operations. The ROI Pooling operation involves two quantization of a decimal. After two quantifications, there is a certain deviation between the selection box and the original position. The ROI Align operator cancels the double integer operation and retains the decimal. For each decimal position, bilinear interpolation method is used to obtain the value of the feature graph whose coordinates are floating-point numbers, thus transforming the whole feature aggregation process into a continuous operation [33]. This avoids the bias of candidate bounding boxes in different feature extraction stages. The whole feature aggregation process after ROI Align replaces ROI Pooling is shown in Fig. 2. ROI Align eliminates the misalignment caused by quantization in ROI Pooling, leading to more accurate feature extraction, which is especially crucial for detecting fine-grained anatomical structures of the scapula.

The fracture location label file and JPG format image data converted from DICOM format data were imported into the CNN algorithm framework. The detection frame information obtained by the model is converted into the coordinate information on the original image, and the redundant prediction frame is cleared by the intersection ratio threshold detection and non-maximum suppression. After the first model construction, the recognition image of scapular fracture was obtained (Fig. 3).

After the initial modeling, the accuracy of recognition is not ideal. In order to optimize the model, two times of modeling were carried out. The model optimization process involves selecting the appropriate hyperparameters to achieve the best performance. Mesh search and random search techniques are used to optimize the parameters, aiming to balance training speed and model accuracy [34]. We also performed K-break cross-validation (k = 5) to evaluate the generalization ability of

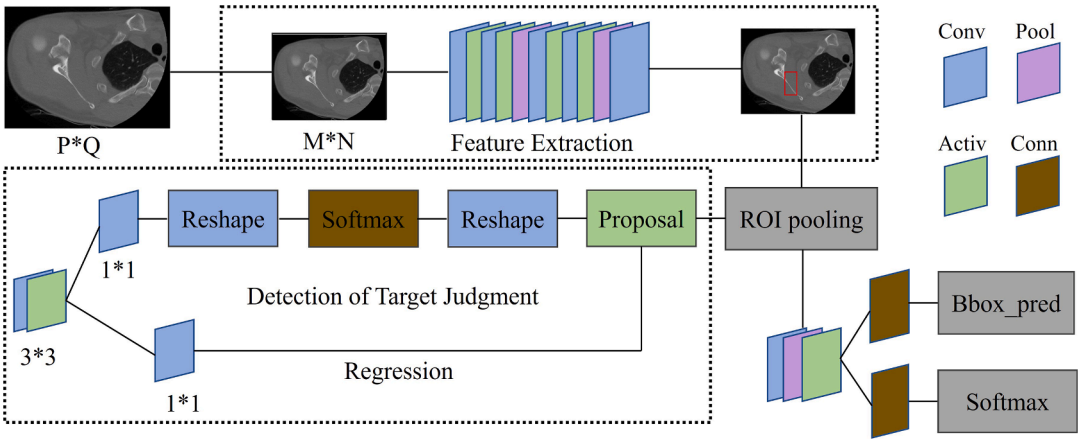

Fig. 1. Workflow diagram of object detection for Faster R-CNN.

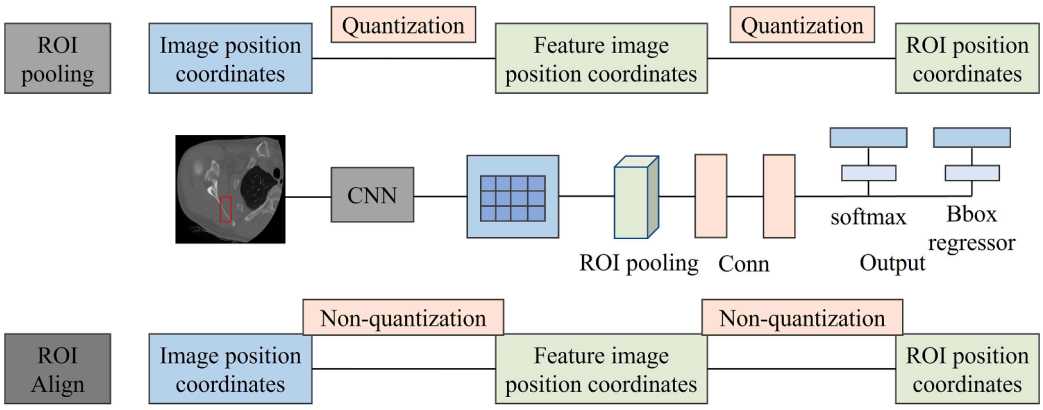

Fig. 2. Feature aggregation flow chart after ROI Pooling is replaced by ROI Align.

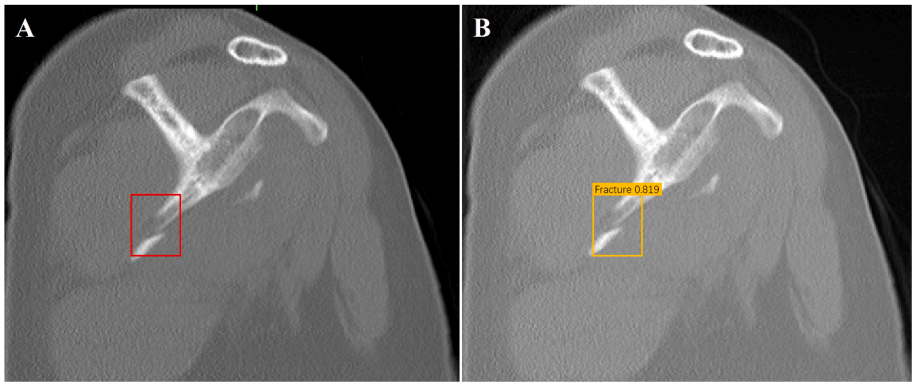

Fig. 3. The scapular fracture labeling and recognition images obtained after the initial modeling. A: Fracture labeling image. B: The model recognizes fracture images.

the model under different hyperparameter configurations, ensuring a consistent performance of the model over a diverse dataset, thereby improving the predictive power of the model (Fig. 4). The form of the standard binary cross entropy loss function is:

$$L_{(p,y)} = -[y\log(p) + (1-y)\log(1-p)] \tag{1}$$

After splitting the function, define a new variable pt to express the form of the function:

$$p_t = \begin{cases} py = 1 \\ 1 - py = 0 \end{cases} \tag{2}$$

The binary cross entropy loss function is succinctly defined as:

$$L_{(p,y)} = -\log(p_t) \tag{3}$$

Softmax classification function is:

$$P_i = \frac{e^{x_i}}{\sum_j e^{x_j}} \tag{4}$$

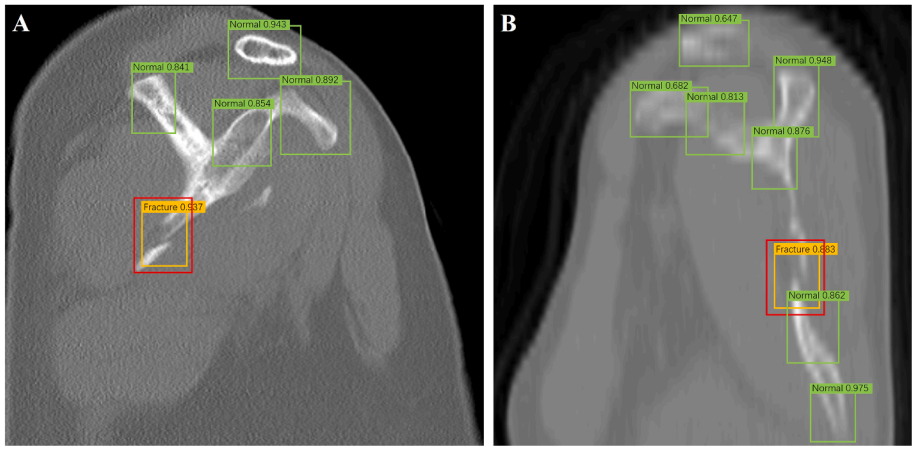

Fig. 4. Recognition image of scapular fracture after model optimization. The red wire frame is the fracture area outlined by the medical expert. The yellow wire frame is the fracture area identified by the prediction model. The green wire frame is the nmal area identified by the prediction model.

where x represents the unnormalized calculated value of the last classified output layer. Show the final class probability calculation value. I indicates the class of the calculated object

In summary, the standard cross entropy loss function based on Softmax classification is as follows:

$$P_t = \frac{e^{x[cls]}}{\sum_j e^{x[j]}} \tag{5}$$

$$L(\mathrm{x},\ \mathrm{cls}) = -\log\frac{e^{x[cls]}}{\sum_j e^{x[j]}} \tag{6}$$

To solve the imbalance problem of positive and negative samples, the usual practice is to introduce the weight factor α. When the class label of the sample is positive, the weight factor given is α. When the class label is negative, the weight factor is 1-α. It can be represented by α_t.

$$\alpha_t = \begin{cases} \alpha y = 1 \\ 1 - \alpha y = 0 \end{cases} \tag{7}$$

At this time, the cross entropy loss function based on Softmax classification is:

$$L(\mathrm{x},\ \mathrm{cls}) = -\alpha_t \log\frac{e^{x[cls]}}{\sum_j e^{x[j]}} \tag{8}$$

A new dynamic modulation factor $(1\text{-}p_t)^{\beta}$ was used in this paper to reduce the weight of easily distinguishable samples and to solve the imbalance problem of difficult and easy samples. Finally, the new dynamic modulation cross entropy loss function based on Softmax classification can be expressed as:

$$L(\mathrm{x},\ \mathrm{cls}) = -(1 - P_t)^{\beta} \log\frac{e^{x[cls]}}{\sum_j e^{x[j]}} \tag{9}$$

2.4. Construction of fracture recognition method

Three different methods were used to detect scapular fractures on shoulder CT. Method 1: The medical expert read the film independently, and the intermediate orthopedist read the transverse image independently. Method 2: CNN algorithm model was used to identify scapular fractures. Method 3: The CNN algorithm combined with the orthopedist's radiography to conduct a comprehensive examination of the fracture detection.

The fracture areas detected in each group were recorded, and the scapular CT images of 90 patients were simultaneously reviewed and analyzed by two associate chief physicians who had been engaged in imaging diagnosis for more than 15 years. The physicians perform image analysis according to the interpretation guidelines for scapular fractures, and the orthopedist's level of experience and understanding of different anatomical structures have a significant impact on the identification results. In order to improve the recognition efficiency and accuracy of orthopedic surgeon , we use image enhancement software to adjust the image contrast and enhance the edge. In case of disagreement, a unified diagnosis is reached after discussion and used as the gold standard.

2.5. Evaluation of fracture identification methods

The 95 % confidence interval was calculated using the normal distribution test to evaluate the diagnostic accuracy, sensitivity, specificity, positive and negative prediction rates of three different identification methods. The area under the curve (AUC) area was calculated using the receiver operating characteristic (ROC) curve to assess diagnostic reliability.

2.6. Statistical analysis

The research data were collected, and SPSS 25.0 statistical software was used for statistical analysis. The counting data is represented by [n (%)]. $P < 0.05$ was considered statistically significant.

3. Results

3.1. Efficacy evaluation of fracture recognition model

The diagnostic sensitivity, specificity, positive predictive value and negative predictive value of the CNN algorithm model combined with physician interpretation method for scapular fracture were 95.78, 93.75, 97.9, and 81.74, respectively. The specificity and positive predictive value of the CNN algorithm model combined with medical expert interpretation method are significantly higher than the results of medical expert interpretation and algorithm independent prediction ($P < 0.05$, Table 1).

The AUC curve for scapular fractures identified by CNN algorithm model and doctor group was 0.866 (95 %CI: 0.791 ~ 0.942). The AUC predicted by physician independent interpretation and algorithm independent prediction were 0.787 (95 %CI: 0.702 ~ 0.872) and 0.837 (95 %CI: 0.754 ~ 0.919), respectively. The AUC value of the CNN algorithm model combined with doctor group was significantly higher than that of orthopedist independent interpretation and algorithm independent prediction group, and the difference was statistically significant ($P < 0.05$). Detailed results are shown in Fig. 5.

3.2. Detection rate of fracture area

The recognition results of scapular fractures between six sites by three different fracture recognition methods are shown in Table 2. The body of scapula, neck of scapula, and acromion are the most commonly identified areas of scapular fracture. In addition, the accuracy of the CNN algorithm model combined with orthopedist identification method was 97.78 %, which was significantly higher than the accuracy of orthopedist-independent interpretation (82.95 %) and algorithm-independent prediction (92.05 %) ($P < 0.05$).

4. Discussion

The scapula is a triangular-like flat bone located behind the thorax. It has a complex and irregular anatomy and is the starting or attachment point of many muscles [6]. Due to the particularity of the structure and position of the scapula, the occurrence of fractures and other types of lesions in this part may lead to the dysfunction of the shoulder joint and the upper limb of the patient [3]. If effective treatment is not taken in time, it is easy to lead to irreversible changes such as disability of the affected side of the patient's upper limb, which will affect the daily life and work of the patient, resulting in a decline in the quality of life of the patient [4,35]. The recognition accuracy of different regions of scapula is different, mainly because the anatomical structure of the neck of scapula is complicated and often coexists with the scapula body fracture, which makes the recognition difficulty increased. The overlap of shoulder blades with soft tissues (e.g., muscles) and other bone structures (e.g., ribs, clavicle) further increases the difficulty of image analysis [36]. Timely and effective treatment can accelerate the recovery of patients and reduce the damage of fractures [9,37].

Table 1
Comparison of diagnostic value of three different methods to identify scapular fracture (100%).

Evaluation index	Team			P
	Doctor	Algorithm	Combination	
Sensitivity	77.68	86.90	95.78	<0.05
Specificity	80.65	89.24	93.75	>0.05
Positive predictive value	93.50	96.96	97.90	>0.05
Negative predictive value	47.00	84.54	81.74	<0.05

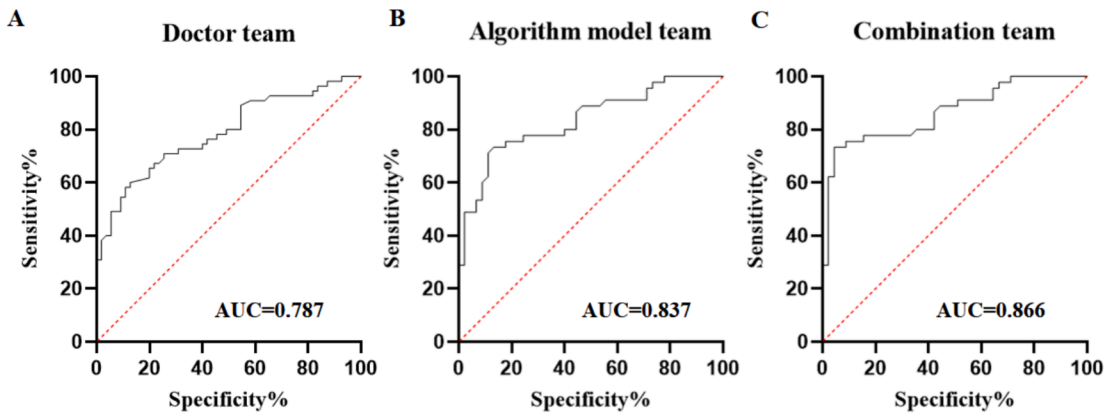

Fig. 5. ROC curves of three different methods for identifying scapular fractures.

Table 2
Comparison of fracture area of three different methods to identify scapular fracture.

Fracture location	Identification method		
	Doctor team	Algorithm team	Combination team
Scapular neck	15	17	18
Coracoid process	9	10	11
Glenoid	5	6	7
Acromion	10	11	12
Scapular body	27	29	30
Scapular spine	7	8	10
Accuracy	82.95 %	92.05 %	97.78 %

In this study, a diagnostic model of scapular fracture was constructed based on the CNN algorithm. The model enables fully automated, end-to-end imaging diagnosis of scapular fractures and provides fracture recognition probabilities [18]. The CNN model can recognize the common DICOM format file of the CT image and has high universality [38]. At the same time, the model is simple to operate and the recognition speed is fast [39]. The auxiliary diagnosis of a scapular fracture can not only improve the identification efficiency but also the interpretation results are not affected by human factors [12,40,41,42]. It avoids missing diagnoses and misdiagnoses caused by manual interpretation due to lack of experience and other reasons.

Based on the included CT data of 90 scapular fractures, we constructed three different fracture identification methods. In terms of diagnostic efficacy, the sensitivity, specificity, positive predictive value, and negative predictive value of scapular fracture were the highest in the combination of then CNN algorithm model and physician interpretation method. In addition, the specificity and positive predictive value of the algorithm model recognition method were significantly higher than the prediction results of orthopedist-independent interpretation ($P < 0.05$). It shows that the CNN model has robust performance in the interpretation of different CT image materials, so it can obtain more reliable results than manual interpretation. The AUC curve for scapular fractures identified by the algorithm model and the doctor team was 0.866 (95 % CI: 0.791 ~ 0.942). The AUC predicted by physician independent interpretation and algorithm independent prediction were 0.787 (95 % CI: 0.702 ~ 0.872) and 0.837 (95 % CI: 0.754 ~ 0.919), respectively. The AUC value of the algorithm model combined with the doctor group was significantly higher than that of the doctor independent interpretation and algorithm independent prediction group, and the difference was statistically significant ($P < 0.05$). Guermazi et al, [43] demonstrated that AI-assisted examination can improve the sensitivity of fracture diagnosis and even improve the specificity of fracture detection by radiologists and non-radiologists, but it does not extend the reading time. The diagnostic results of the algorithm model combined with doctors have higher accuracy, sensitivity, and specificity than those of the independent identification method. Therefore, AI-model-assisted diagnosis has the potential to minimize the gap in scapular fracture recognition between less experienced physicians and more experienced physicians [44]. It can be seen that the CNN algorithm model significantly improves the diagnostic accuracy of radiologists in the detection of scapular fractures. It is an effective way for doctors to reduce the missed diagnosis of rib scapula fracture by carefully reading the film with the help of the CNN algorithm model.

Among the three different detection methods, the accuracy of the algorithm model combined with the orthopedist-identification method was 97.78 %, the accuracy of the orthopedist independent interpretation was 82.95 %, and the accuracy of the CNN algorithm recognition was 92.05 %. The results showed that the ability of orthopedic surgeon to detect fractures was insufficient, which may be related to the lack of sufficient knowledge of orthopedist to distinguish minor fractures. Previous studies have shown that the higher the accuracy, the lower the false positive rate of fracture recognition by the model [45]. It is considered that the main reason for the false-positive results in this study model is that the number of some types of fractures is small and the feature learning is insufficient in the learning process [46]. In the training process, the model confused the non-fracture image with the fractured image, and identified the non-fracture site, resulting in false positives [47]. In addition, in the practical application of the CNN model, all the DICOM format data of the evaluated shoulder CT will be input into the model [48]. Some of the scapulas at the sagittal level showed similar walking and morphological features to the cross-sectional scapulas and were identified as fractures [49].

There are some limitations in this study. First of all, the number of samples is relatively small, which makes it difficult to further improve the algorithm recognition accuracy. In the future, better algorithm models can be trained by increasing the sample size to achieve better accuracy. Secondly, the CNN network structure can be further optimized to increase the depth of the CNN network structure, which may enhance the learning ability of the algorithm to recognize the model and obtain a better training model. In future implementations, we will utilize more advanced algorithms and models from the cybernetical intelligence perspective [50] in order to improve our target detection performance.

5. Conclusion

In summary, the intelligent recognition model of scapular fracture based on the CNN algorithm was established in this study, and it was confirmed that this model had excellent performance in recognizing scapular fracture CT images. This model can assist clinicians in improving their diagnostic ability and accuracy in locating scapular fractures on CT images.

CRediT authorship contribution statement

Qiong Fang: Writing – original draft, Methodology, Conceptualization. **Anhong Jiang:** Software, Resources. **Meimei Liu:** Writing – review & editing, Project administration. **Sen Zhao:** Visualization, Methodology.

Declaration of competing interest

The authors declare that they have no known competing financial interests or personal relationships that could have appeared to influence the work reported in this paper.

Acknowledgement

This work was supported by the Natural Science Research Project of Anhui Colleges and Universities (KJ2021A1259, KJ2021A1272).

Ethics Statement

This study was approved by the Ethics Committee of Anhui Medical College (2025-LLBG-003).

References

[1] F. Xiang, Y. Xiao, D. Wei, et al., Finite element analysis of a novel anatomical locking plate for scapular neck fracture, J. Orthop. Surg. Res. 18 (1) (2023) 262.
[2] H.M. Yimam, R. Dey, P.A. Rachuene, et al., Identification of recurring scapular fracture patterns using 3-dimensional computerized fracture mapping, J. Shoulder Elbow Surg. 31 (3) (2022) 571–579.
[3] K. Sonawane, J. Balavenkatasubramanian, H. Dixit, et al., Regional anesthesia for scapular fracture surgery: An educational review of anatomy and techniques, Reg. Anesth. Pain Med. 46 (4) (2021) 344–349.
[4] C. Libby, N. Frane, T.P. Bentley, Scapula fracture. *Statpearls*. Treasure Island (FL) ineligible companies. Disclosure: Nicholas Frane declares no relevant financial relationships with ineligible companies. Disclosure: Thomas Bentley declares no relevant financial relationships with ineligible companies. StatPearls Publishing. Copyright © 2024, StatPearls Publishing LLC.; 2024.
[5] J. Bartoníček, O. Naňka, History of diagnostics and treatment of scapular fractures in children and adolescents and its clinical importance, Arch. Orthop. Trauma Surg. 142 (6) (2022) 1067–1074.
[6] D.N. Reed, J.T. Frix, Scapular stress fracture of the inferior angle in an adolescent swimmer, Orthopedics 46 (4) (2023) e249–e252.
[7] G.C.S. Smith, P. Geelan-Small, M. Sawang, A predictive model for the critical shoulder angle based on a three-dimensional analysis of scapular angular and linear morphometrics, BMC Musculoskelet. Disord. 23 (1) (2022) 1006.
[8] J.C.E. Donders, J. Prins, P. Kloen, et al., Three-dimensional topography of scapular nutrient foramina, Surg. Radiol. Anat. 42 (8) (2020) 887–892.
[9] T. Matsuo, F. Morita, D. Tani, et al., Anatomical variation of habitat-related changes in scapular morphology, Anat. Histol. Embryol. 48 (3) (2019) 218–227.
[10] S. Du, R. Xu, L. Li, Modeling and Analysis of Multiproduct Multistage Manufacturing System for Quality Improvement, IEEE T. Syst. Man Cy. 48 (5) (2018) 801–820.
[11] K. Wang, G. Li, S. Du, L. Xi, T. Xia, State space modelling of variation propagation in multistage machining processes for variable stiffness structure workpieces, Int. J. Prod. Res. 59 (13) (2021) 4033–4052.
[12] G. Li, S. Du, B. Wang, J. Lv, Y. Deng, High Definition Metrology-Based Quality Improvement of Surface Texture in Face Milling of Workpieces With Discontinuous Surfaces, J. Manuf. Sci. Eng. 144 (3) (2022) 031001.
[13] G. Li, S. Du, D. Huang, C. Zhao, Y. Deng, Dynamics Modeling-Based Optimization of Process Parameters in Face Milling of Workpieces With Discontinuous Surfaces, J. Manuf. Sci. Eng. 141 (10) (2019) 101009.
[14] Y. Shao, Y. Yin, S. Du, L. Xi, A Surface Connectivity Based Approach for Leakage Channel Prediction in Static Sealing Interface, J. Tribol. 141 (6) (2019) 062201.
[15] K.K.L. Wong, Automatic target recognition based on Cross-plot, PLoS ONE 6 (9) (2011) e25621.
[16] X. Lin, Z. Yan, Z. Kuang, et al., Fracture r-cnn: An anchor-efficient anti-interference framework for skull fracture detection in ct images, Med. Phys. 49 (11) (2022) 7179–7192.
[17] H.C. Breit, A. Varga-Szemes, U.J. Schoepf, et al., Cnn-based evaluation of bone density improves diagnostic performance to detect osteopenia and osteoporosis in patients with non-contrast chest ct examinations, Eur. J. Radiol. 161 (2023), 110728.
[18] J. Prijs, Z. Liao, M.S. To, et al., Development and external validation of automated detection, classification, and localization of ankle fractures: Inside the black box of a convolutional neural network (cnn), Eur. J. Trauma Emerg. Surg. 49 (2) (2023) 1057–1069.
[19] T. Yoda, S. Maki, T. Furuya, et al. Automated differentiation between osteoporotic vertebral fracture and malignant vertebral fracture on mri using a deep convolutional neural network. Spine (Phila Pa 1976). 2022, 47(8): E347-e352.
[20] Y. Cha, J.T. Kim, C.H. Park, et al., Artificial intelligence and machine learning on diagnosis and classification of hip fracture: systematic review, J. Orthop. Surg. Res. 17 (1) (2022) 520.
[21] L. Tanzi, A. Audisio, G. Cirrincione, et al., Vision transformer for femur fracture classification, Injury 53 (7) (2022) 2625–2634.
[22] J. Shi, Y. Ye, D. Zhu, L. Su, Y. Huang, J. Huang, Automatic segmentation of cardiac magnetic resonance images based on multi-input fusion network, Comput. Meth. Prog. Bio. 209 (2021) 106323.
[23] Y. Ye, J. Shi, D. Zhu, L. Su, J. Huang, Y. Huang, Management of medical and health big data based on integrated learning-based health care system: A review and comparative analysis, Comput. Meth. Prog. Bio. 209 (2021) 106293.
[24] K.K.L. Wong, Z. Sun, J. Tu, S.G. Worthley, J. Mazumdar, D. Abbott, Medical image diagnostics based on computer-aided flow analysis using magnetic resonance images, Comput. Med. Imag. Grap. 36 (7) (2012) 527–541.
[25] K.K.L. Wong, R.M. Kelso, S.G. Worthley, P. Sanders, J. Mazumdar, D. Abbott, Medical imaging and processing methods for cardiac flow reconstruction, J. Mech. Med. Biol. 9 (1) (2009) 1–20.
[26] S.C. Cheung, K.K.L. Wong, G.H. Yeoh, W. Yang, J. Tu, R. Beare, T. Phan, Experimental and numerical study on the hemodynamics of stenosed carotid bifurcation, Australas Phys. Eng. Sci. Med. 33 (4) (2010) 319–328.
[27] M. Zhao, Y. Wei, K.K.L. Wong, A Generative Adversarial Network technique for high-quality super-resolution reconstruction of cardiac magnetic resonance images, Magn. Reson. Imaging 85 (2022) 153–160.
[28] K. Zhao, P. Dai, P. Xiao, Y. Pan, L. Liao, J. Liu, X. Yang, Z. Li, Y. Ma, J. Liu, Z. Zhang, S. Li, H. Zhang, S. Chen, F. Cai, Z. Tan, Automated segmentation and source prediction of bone tumors using ConvNeXtv2 Fusion based Mask R-CNN to identify lung cancer metastasis, J. Bone Oncol. 48 (2024) 100637.
[29] X. Deng, Y. Zhu, S. Wang, Y. Zhang, H. Han, D. Zheng, Z. Ding, K.K.L. Wong, CT and MRI Determination of Intermuscular Space within Lumbar Paraspinal Muscles at Different Intervertebral Disc Levels, PloS one 10 (10) (2015) e0140315.
[30] G. Cui, R. Wang, D. Wu, Y. Li, Semi-supervised Multi-view Clustering based on NMF with Fusion Regularization, ACM Trans. Knowl. Discov. Data 18 (6) (2024) 157.
[31] H. Lei, H. Huang, B. Yang, G. Cui, R. Wang, D. Wu, Y. Li, TCSA: A Text-Guided Cross-View Medical Semantic Alignment Framework for Adaptive Multi-view Visual Representation Learning, Bioinform. Res. Appl. (2023) 136–149.
[32] G. Cui, D. Wu, Y. Li, J. Li, Layer-wise normalized deep incomplete multiview nonnegative matrix factorization, Pattern Recogn. 158 (2025) 111010.
[33] A. Yabu, M. Hoshino, H. Tabuchi, et al., Using artificial intelligence to diagnose fresh osteoporotic vertebral fractures on magnetic resonance images, Spine J. 21 (10) (2021) 1652–1658.
[34] K.K.L. Wong. Cybernetical Intelligence: Engineering Cybernetics with Machine Intelligence, Wiley-IEEE Press, Hoboken, New Jersey, 2023.
[35] K.A. Mahendraraj, J. Abboud, A. Armstrong, et al., Predictors of acromial and scapular stress fracture after reverse shoulder arthroplasty: A study by the ases complications of rsa multicenter research group, J. Shoulder Elbow Surg. 30 (10) (2021) 2296–2305.
[36] A.E.J. Bulstra, R.M.A. Al-Dirini, A. Turow, et al., The influence of fracture location and comminution on acute scaphoid fracture displacement: Three-dimensional ct analysis, J. Hand Surg. Eur. 46 (10) (2021) 1072–1080.
[37] I. Fleps, E.F. Morgan, A review of ct-based fracture risk assessment with finite element modeling and machine learning, Curr. Osteoporos. Rep. 20 (5) (2022) 309–319.
[38] Y.C. Shu, Y.C. Lo, H.C. Chiu, et al., Deep learning algorithm for predicting subacromial motion trajectory: dynamic shoulder ultrasound analysis, Ultrasonics 134 (2023), 107057.
[39] T.H. Yang, M.H. Horng, R.S. Li, et al., Scaphoid fracture detection by using convolutional neural network, Diagnostics (basel) 12 (4) (2022).
[40] S. Mutasa, S. Varada, A. Goel, et al., Advanced deep learning techniques applied to automated femoral neck fracture detection and classification, J. Digit. Imaging 33 (5) (2020) 1209–1217.
[41] J. Shi, Y. Ye, D. Zhu, L. Su, Y. Huang, J. Huang, Comparative analysis of pulmonary nodules segmentation using multiscale residual U-Net and fuzzy C-means clustering, Comput. Meth. Prog. Bio. 209 (2021) 106332.
[42] J. Shi, Y. Ye, H. Liu, D. Zhu, L. Su, Y. Chen, Y. Huang, J. Huang, Super-resolution reconstruction of pneumocystis carinii pneumonia images based on generative confrontation network, Comput. Meth. Prog. Bio. 215 (2022) 106578.
[43] A. Guermazi, C. Tannoury, A.J. Kompel, et al., Improving radiographic fracture recognition performance and efficiency using artificial intelligence, Radiology 302 (3) (2022) 627–636.
[44] Q.Q. Zhou, J. Wang, W. Tang, et al., Automatic detection and classification of rib fractures on thoracic ct using convolutional neural network: accuracy and feasibility, Korean J. Radiol. 21 (7) (2020) 869–879.
[45] Q.Q. Zhou, Z.C. Hu, W. Tang, et al., Precise anatomical localization and classification of rib fractures on ct using a convolutional neural network, Clin. Imaging 81 (2022) 24–32.
[46] G. Kitamura, C.Y. Chung, B.E. Moore 2nd, Ankle fracture detection utilizing a convolutional neural network ensemble implemented with a small sample, de novo training, and multiview incorporation, J. Digit. Imaging 32 (4) (2019) 672–677.
[47] S. Vinayahalingam, N. van Nistelrooij, B. van Ginneken, et al., Detection of mandibular fractures on panoramic radiographs using deep learning, Sci. Rep. 12 (1) (2022) 19596.

[48] R.Y.L. Kuo, C. Harrison, T.A. Curran, et al., Artificial intelligence in fracture detection: A systematic review and meta-analysis, Radiology 304 (1) (2022) 50–62.
[49] S.K. Sundararajan, B. Sankaragomathi, D.S. Priya, Deep belief cnn feature representation based content based image retrieval for medical images, J. Med. Syst. 43 (6) (2019) 174.
[50] K.K.L. Wong, K. Chipusu, M.A. Ashraf, A.W.H. Ip, C.W.J. Zhang, In-space cybernetical intelligence perspective on informatics, manufacturing and integrated control for the space exploration industry, J. Ind. Inf. Integr. 42 (2024) 100724.